SEISMIC PERFORMANCE OF PRECAST HOLLOW-CORE FLOORS WITH MODERN DETAILING: A CASE STUDY

Mostafa, M.[1,*], Hogan, L.[2], Elwood, K.J.[3]

ABSTRACT

This paper describes the observed seismic performance of precast hollow-core floors from an instrumented building subjected to design-level ground shaking during the 2016 Kaikōura earthquake. The hollow-core floors in the building incorporated the detailing requirements of the current design standard, NZS3101:2006-A3, which were intended to suppress undesirable failure modes such as loss of support, negative moment failure, positive moment failure, and rupture of non-ductile topping mesh. The structural system was extensively surveyed to document the severity and distribution of the damage sustained in the flooring system. Furthermore, the building response during the earthquake was reconstructed from the acceleration records obtained from instruments installed throughout the building to estimate the demands on the floor units. While the failure modes that the NZS 3101 hollow-core detailing was designed to suppress were not observed in the building, the damage survey showed unexpected poor performance of hollow-core floor units seated within the plastic hinge regions of the supporting beams and in line with columns, which are referred to as "beta units". It was found that beta units incurred more damage than units seated outside the plastic hinge zone. The susceptibility of these beta units to sustain severe damage is neither recognised in the current design standard, NZS3101:2006-A3, nor in the technical proposal aiming to revise the Assessment Guidelines C5 (Yellow Chapter).

1 INTRODUCTION

The susceptibility of precast hollow-core floors to sustain severe damage under seismic actions has been recognised and extensively investigated since the early 2000s, as summarised in Corney et al. (2021) and Puranam et al. (2021). Through these previous investigations, improvements to the floor-to-support connection details have been developed and proof tested to address the potential failure mechanisms that have been identified in previous research (Lindsay 2004; MacPherson 2005). Although extensive laboratory tests have been undertaken to investigate the performance of these floors, the tests setups that were used represent a simplified version of real-life structures and lack the ability to replicate all of the deformation and inertial demands present in a building during an earthquake. Discrepancies between the observed building performance and laboratory specimen behaviour are attributed to many factors, such as size effects, 3D interaction between multiple structural components, and dynamic characteristics of the earthquake. Accordingly, learning from structural damage observations in previous earthquakes has played a pivotal role in enhancing the understanding of the performance of different structural components when incorporated in a structural system. These damage observations have also led to the progressive improvement of design standards and building codes. Recognising the significance and benefits of learning from the response of real buildings under earthquakes, multiple buildings have been instrumented throughout New Zealand over the years to capture the seismic demand and the response of these structures (Uma et al. 2011; Van Houtte et al. 2017).

The 2016 Kaikōura earthquake resulted in seismic demands exceeding the design level demands for buildings with periods of 1-2 s at some locations in Wellington (Henry et al. 2017). The building investigated in this paper was one of six instrumented buildings in Wellington and the Upper South Island that experienced shaking in the Kaikōura earthquake. The building sustained widespread damage after the earthquake, with extensive damage to the floors resulting in the demolition of the building. As part of the demolition programme all non-structural components were removed prior to the structure's demolition, leaving the damaged structure exposed. The structure was extensively surveyed to document the severity and distribution of damage resulting from the earthquake. Detailed damage documentation and crack mapping were undertaken to capture the structural damage sustained in the building. Furthermore, the data recorded from the instrumentation

PAPER CLASS & TYPE: GENERAL REFEREED

1 Ph.D. Candidate, University of Auckland
2 Lecturer, University of Auckland
3 Professor, University of Auckland
** mohamed.mostafa@auckland.ac.nz*

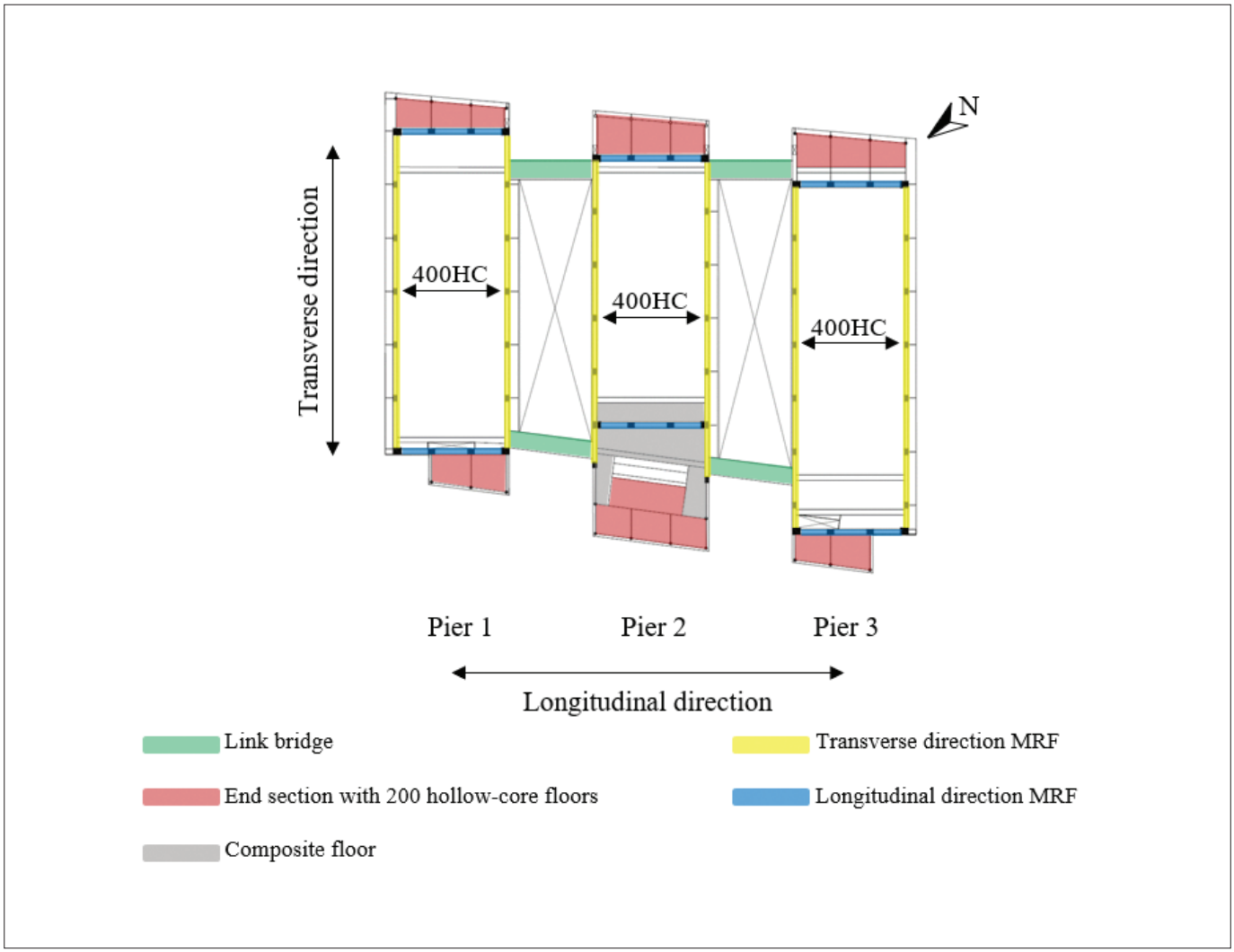

Figure 1: Schematic for building layout

installed in the building were used to provide an estimate of drift demand, which has been correlated with observed damage. This paper aims to highlight the key floor damage observations in the building and potential implications this observed damage has on the current design standard, NZS3101:2006 (Standards New Zealand 2017), as well as the technical proposal aiming to revise the Assessment Guidelines C5 (MBIE et al. 2018).

2 BUILDING DESCRIPTION

The building investigated was a commercial office building with ductile reinforced concrete moment resisting frames and a precast flooring system constructed in 2009. The building was located on the waterfront in Wellington. The layout of the building consisted of three seismically linked buildings referred to as "piers" that were connected via composite steel-concrete pedestrian 'link bridges' and separated by two atrium spaces, as is shown in Figure 1. Pier 1 and Pier 3 were five stories tall, while Pier 2 had an additional sixth storey constructed of steel to house mechanical equipment. The link bridges were designed with sufficient strength to tie the piers together in the longitudinal direction. In addition to the link bridges at each floor, Piers 2 and 3 were connected with a floor diaphragm at Level 1. Ductile reinforced concrete perimeter moment resisting frames (MRFs) were used to serve both the gravity load carrying system as well as the lateral load resisting system. The frames consisted of precast concrete beams with in-situ columns and joint elements designed and detailed for high ductility in both principal directions of the building.

The spacing between the column centrelines in the longitudinal frame varied between 5.4 to 6.0 m, whereas in the transverse frames the columns were 8.1 m apart. A precast, prestressed hollow-core floor system was used to span approximately 17 m in the longitudinal direction of the building between the perimeter frames. The typical floor system was a 400 mm thick hollow-core slab (HC) with a cast-in-situ 100 mm topping layer

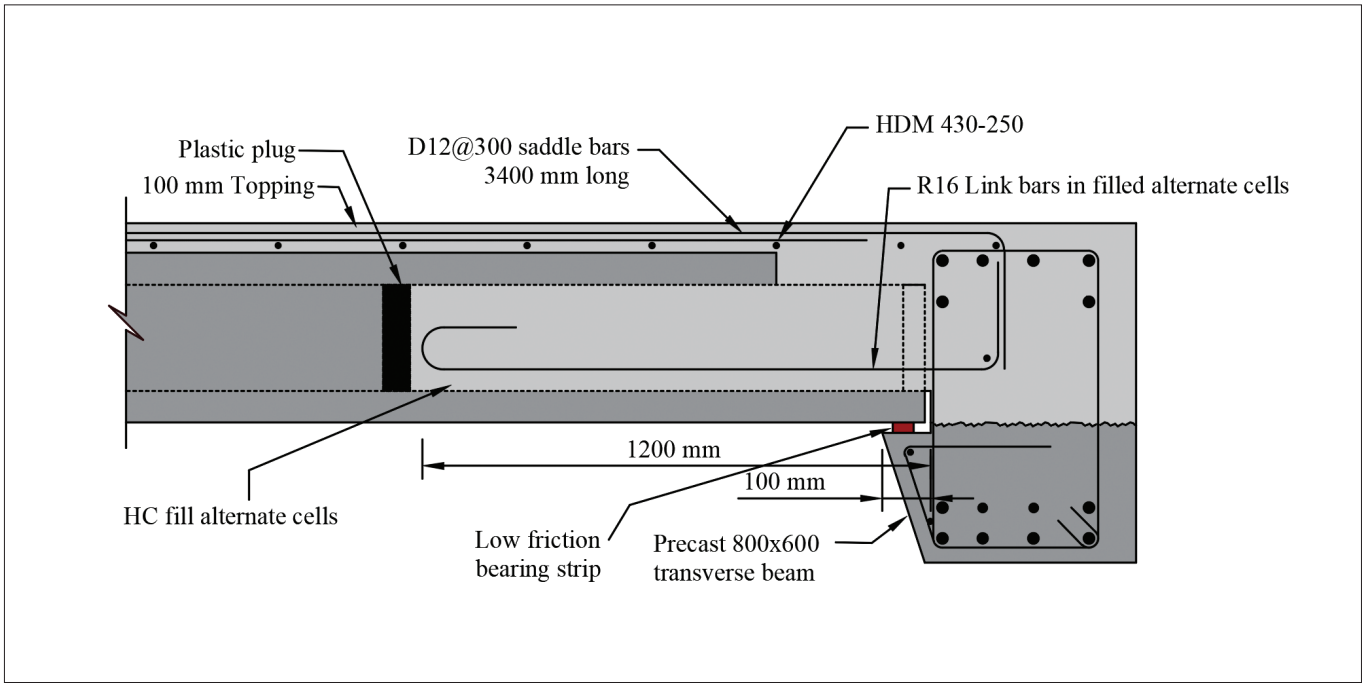

Figure 2: Schematic of floor to beam connection detail (dark grey colour indicates precast portion)

reinforced with ductile mesh (HDM-430-300). Figure 2 shows a typical floor connection detail. The connection detail used in the building was consistent with C18.6.6(e) of NZS3101:2006-A3, which is referenced within clause 3.1.1 of B1/VM1 (MBIE 2021) and hence can be considered a deemed-to-comply solution meeting the performance objectives of the Building Code. The hollow-core units had 100 mm specified seating length with a 50 mm wide low friction bearing strip. Every second cell of the unit was filled, and a 16 mm plain round bar was cast in these filled cells and tied back to the supporting beam. In-situ "link slabs" were used to accommodate deformation incompatibilities between the floor and frame in locations where hollow-core slabs run parallel to multiple-bay frames.

At the north and south ends of each pier, steel frames and 200 mm thick hollow-core slabs were used for the floor system (Figure 1). Composite flooring was used in the area around the lift shafts in Pier 2. Furthermore, 175 mm thick precast cantilever floors were used for edge walkways in the building. At roof level, cold-formed purlins were supported by structural steel portal frames. The ground level used a slab-on-grade concrete floor. NZS3101:2006 was used to design the concrete moment frames and the floors.

3 GROUND MOTION

The magnitude 7.8 Kaikoura earthquake occurred along the east coast of the upper South Island on 14 November 2016 at 12:02 a.m. local time, with an epicentre approximately 20 km south of the Hope fault, at a depth of 15 km (GeoNet 2016; Hamling et al. 2017). The event included multiple fault segment ruptures, which propagated northeast from North Canterbury with significant energy being propagated towards the Wellington region (Bradley et al. 2017; Kaiser et al. 2017). The approximate location of the source zone and rupture propagation direction are indicated in Figure 3a. Despite Wellington's distance from the source, strong shaking was experienced in some parts of the city. This shaking intensity is mainly attributed to the amplification of ground motion by the deep sediments underlying the city as well as being in the path of the focussed seismic waves propagating in the direction of rupture. For the building investigated, a free field sensor located at the building site showed local site amplification effects due to deep soil deposits, which resulted in strong energy content in the 1–2 s period range, as shown in Figure 3b. For comparison purposes, the spectral values for the Wellington CBD, soil class D based upon NZS 1170.5:2004 (Standards New Zealand 2016) was plotted for both the ultimate limit state (ULS) and serviceability limit state (SLS) against the 5% damped response spectra of the ground motion recorded with the free-field instrument located at the building site along the longitudinal and transverse axes of the building. The

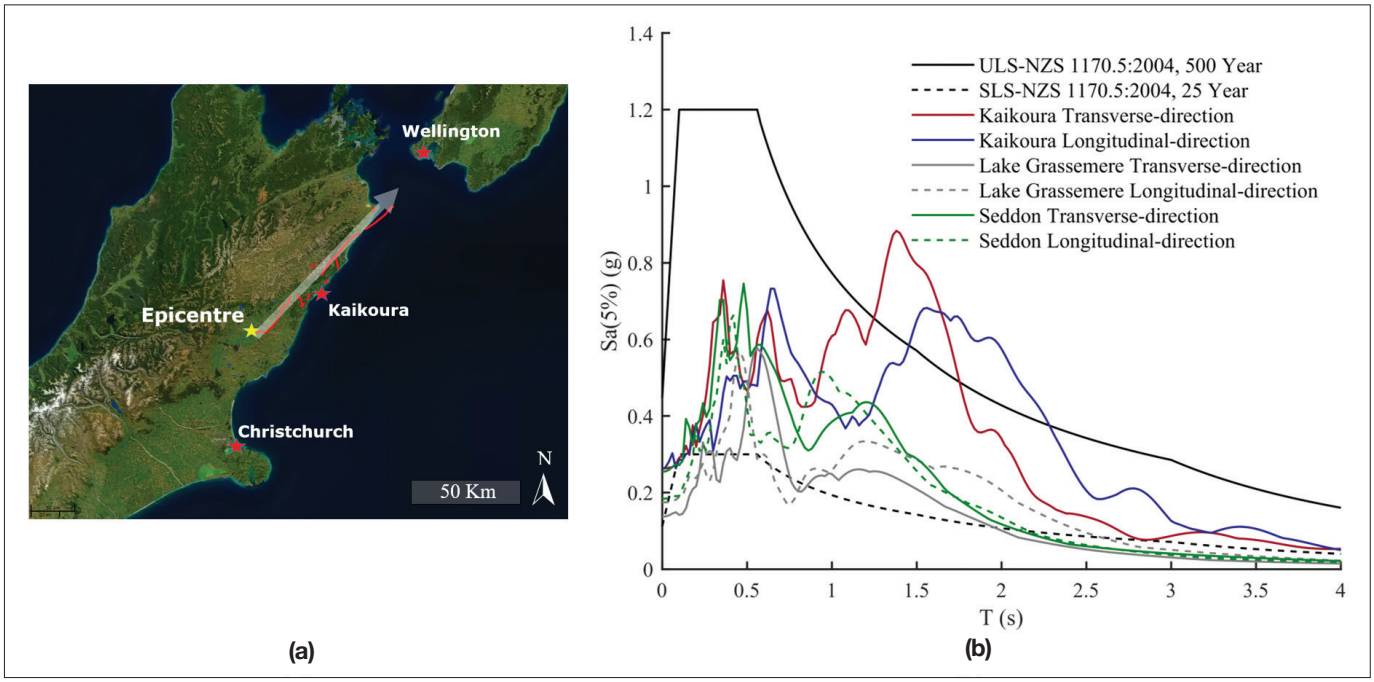

Figure 3: (a) approximate location of Kaikōura earthquake epicentre and faults ruptures according to Hamling et al., (2017) (b) 5% damped spectral accelerations of the free-field ground motions rotated to coincide with the longitudinal and transverse axes of the building and the ULS and SLS design response spectra according to NZS1170.5:2004.

moderately long duration of the ground motion alongside the high energy content in the 1-2 s period range led to floor accelerations reaching about 0.8g and inter-storey drifts reaching about 1.8%, which resulted in damage to different structural components in the building, including spalled concrete in columns and beams, cracks in beams, columns and floor slabs at the column joints. It is worth noting that the building was previously subjected to two earthquakes in 2013, the M-6.5 Cook Strait earthquake (GeoNet 2013a) and the M-6.6 Lake Grassmere earthquake (GeoNet 2013b). Following the Cook Strait earthquake (sometimes referred to as the Seddon earthquake), minor structural damage was observed and a significant amount of non-structural damage was observed (Dominion Post 2013).

4 BUILDING RESPONSE

The building response was captured using 14 tri-axial CUSP-M accelerometers (CSI Limited 2017) installed throughout the building, as shown in Figure 4, and one free-field accelerometer was used to capture the local site ground motions. Pier 3 was instrumented with at least one accelerometer in each storey. Sensors 3-11 and sensor 15 were used for levels G to 6 in Pier 3 to monitor the motion at the centre of each level. The fifth floor (ceiling of level 4) of the building was instrumented with five sensors to capture any twisting motion if present.

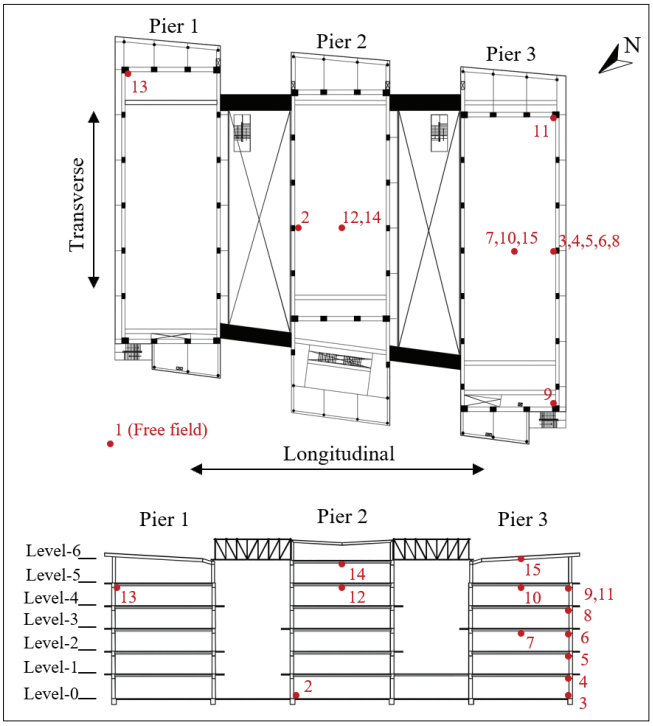

Figure 4: Locations of installed triaxial accelerometers throughout the building

The strong motion data was obtained through the GeoNet instrumentation network (GeoNet 2016) and was then processed based on recommendations from Boore and Bommer (2005) to have the two orthogonal horizontal components of each record coinciding with the longitudinal and transverse direction of the building.

Since Piers 1 and 2 of the building were too sparsely instrumented to be able to reconstruct the response of these portions of the building, only the response of Pier 3 was reconstructed and computed. For each floor level in Pier 3, sensors 3, 4, 5, 6, 8 and 10 were considered to represent the motion of the entire floor, assuming a rigid diaphragm. The peak floor acceleration (PFA) at each level for both transverse and longitudinal directions of the building was computed as the absolute maximum acceleration over the entire time series. As such, these PFA's values could have occurred at different times and directions. The PFA variation along the height of the building for both orthogonal directions of the building are plotted in Figure 5a. A maximum PFA of about 0.8 g was observed at the fifth level in the transverse direction. To compute the inter-storey drifts, the displacement time series for each level was first computed by double integrating the acceleration time series for each level using the software Seismosignal (Seismosoft 2016). Then the inter-storey drift ratio (ISD) time series of each storey was computed as the difference between the derived displacement time series of the upper and lower levels of each storey normalised by the storey height. The peak ISD for each storey was computed as the absolute maximum ISD over the entire time series. Similar to PFA, peak ISD could have also occurred at different instants of time. Figure 5b shows the variation in peak ISD over the building height.

The simplified method of response spectral ratios (McHattie 2013) was used here to estimate the fundamental modal period in each orthogonal direction of the building. The spectral ratio can be calculated as the ratio of the spectral acceleration of the seismic response recorded at a given point in the structure and the spectral acceleration recorded at the ground floor. As shown in Figure 6, the non-dimensional acceleration peaks generally take place around the same period because buildings amplify frequencies close to their modal frequencies. Hence, the period at which response spectral ratios peaks was adopted as an estimate of the fundamental period of building. The fundamental period of vibration for the transverse and longitudinal directions was estimated to be approximately 1.2 s and 1.3 s, respectively. By plotting the deduced periods for both longitudinal and transverse frames against the response spectra (Figure 7), it can be found that the estimated fundamental periods generally match the recorded peak floor acceleration. It is important to note that, although a simple method was used here to estimate the fundamental modal periods, there are more sophisticated methods available that can be used to provide a more refined approximation of the modal properties (Hasan et al. 2018; Peeters and De Roeck 1999).

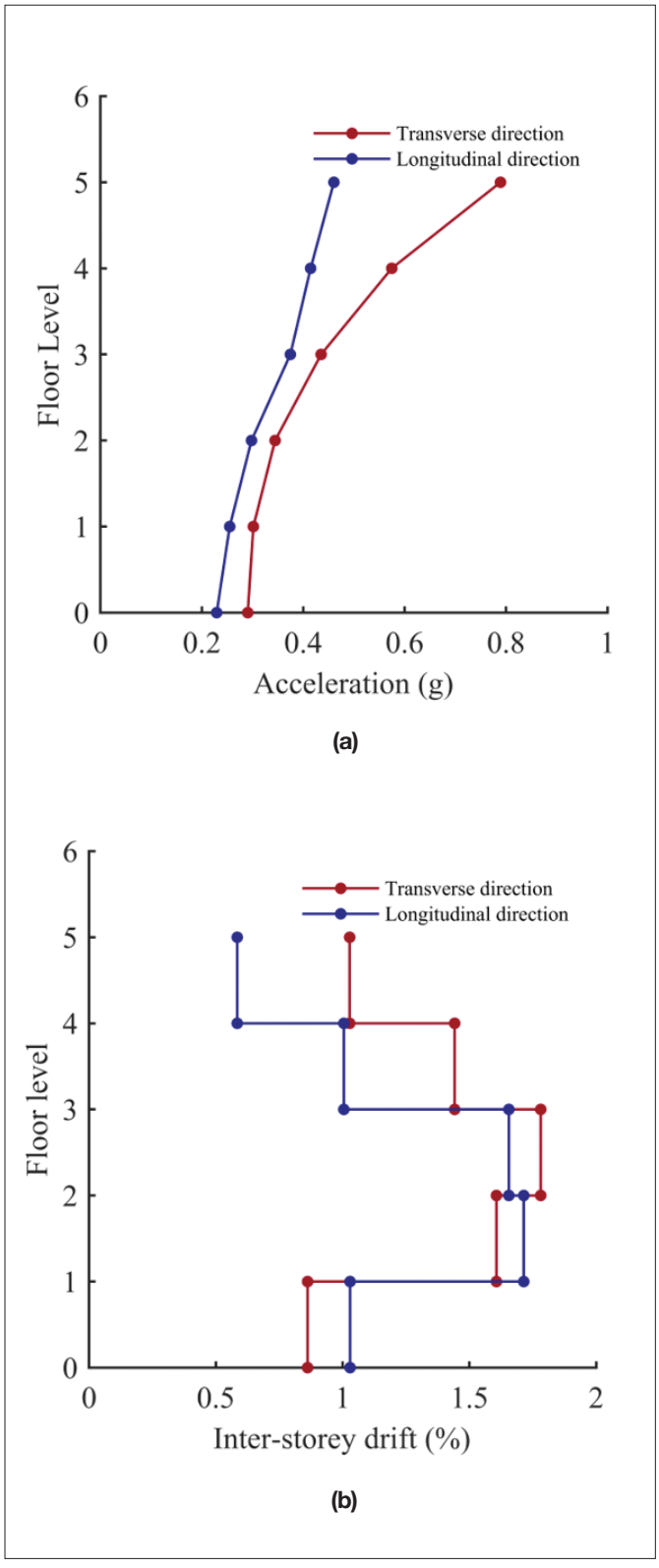

Figure 5: (a) peak floor accelerations (b) peak inter-storey drifts

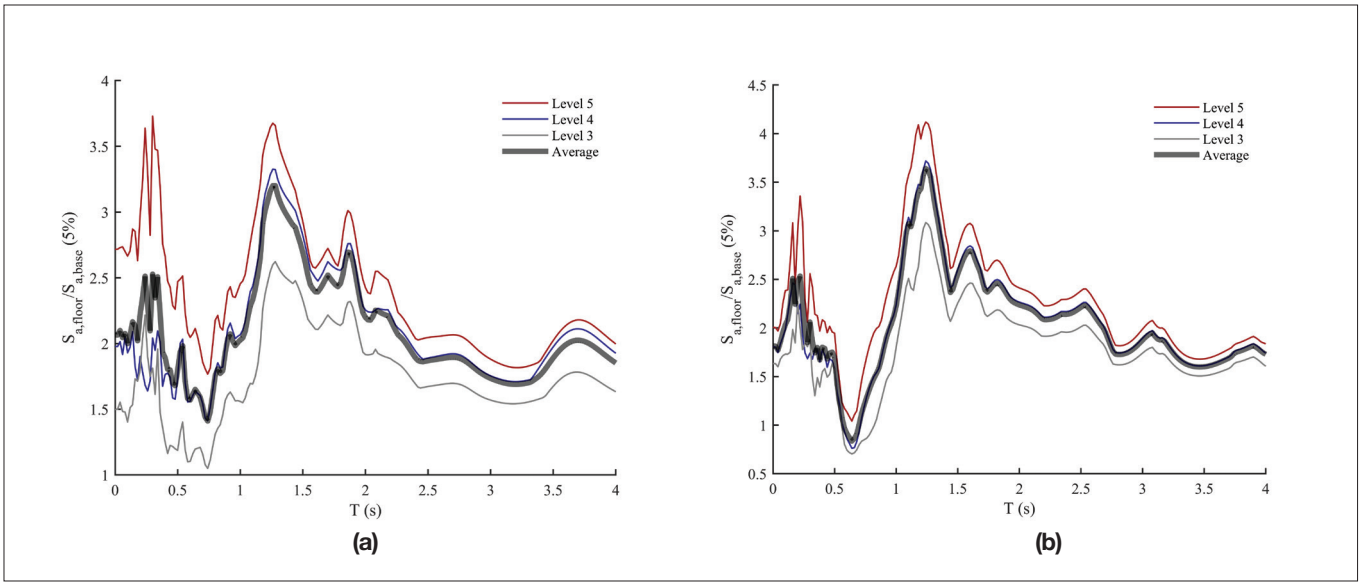

Figure 6: Spectral ratios from the top three storeys' instruments (a) transverse direction (b) longitudinal direction

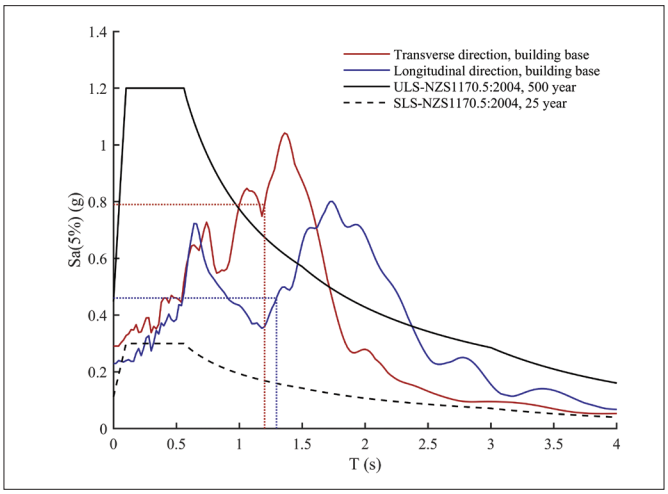

Figure 7: 5% damped response spectra of the building-base ground motions in the transverse and longitudinal directions of the building relative to the 500-year and 25-year return period (NZS 1170.5:2004) elastic design spectra with the fundamental periods inferred from response spectral ratios analysis indicated

5 OBSERVED FLOOR PERFORMANCE

This section summarises the key observations from the damage investigation of the floors. The discussion is limited to the observations of different damage states observed in the building rather than the performance of the building itself. More information regarding the building performance can be found in Siddiqui et al. (2019a) and Siddiqui et al. (2019b). Nevertheless, it is worth noting that the frame damage observed was predominantly concentrated in beam plastic hinge zones, with damage ranging from minor cracking to concrete cover spalling and residual crack widths up to 4 mm. This level of frame damage was generally considered to be repairable. More information regarding the damage sustained in the building can be found in Mostafa et al. 2022b.

The information collected and presented herein is based on extensive damage mapping of the floor units and floor diaphragm (topping). After removing the non-structural elements such as ceilings, carpets, linings and panelling, detailed damage inspections of the floors were undertaken. The extent of floor diaphragm damage was mapped and crack widths were measured. Inspection of the damage sustained in the soffit of the hollow-core floor and reduction in support length due to seating ledge spalling was also conducted.

5.1 TOPPING AND SUPPORT DAMAGE

The damage in the topping of the floors was observed throughout the building. Figure 8 shows one-floor diaphragm damage as an example of the typical damage observed and marked with red lines. The topping damage primarily consisted of longitudinal cracks between adjacent units and some longitudinal cracking within the width of units. These longitudinal cracks had residual widths ranging from 0.3 mm to 7 mm, with larger crack widths typically occurring between units. In the areas adjacent to the columns, concentrated transverse and longitudinal cracking with crack widths ranging from hairline to 4 mm wide were observed. No mesh rupture was observed in the topping as ductile mesh was used.

Support ledge spalling at the columns and plastic hinge

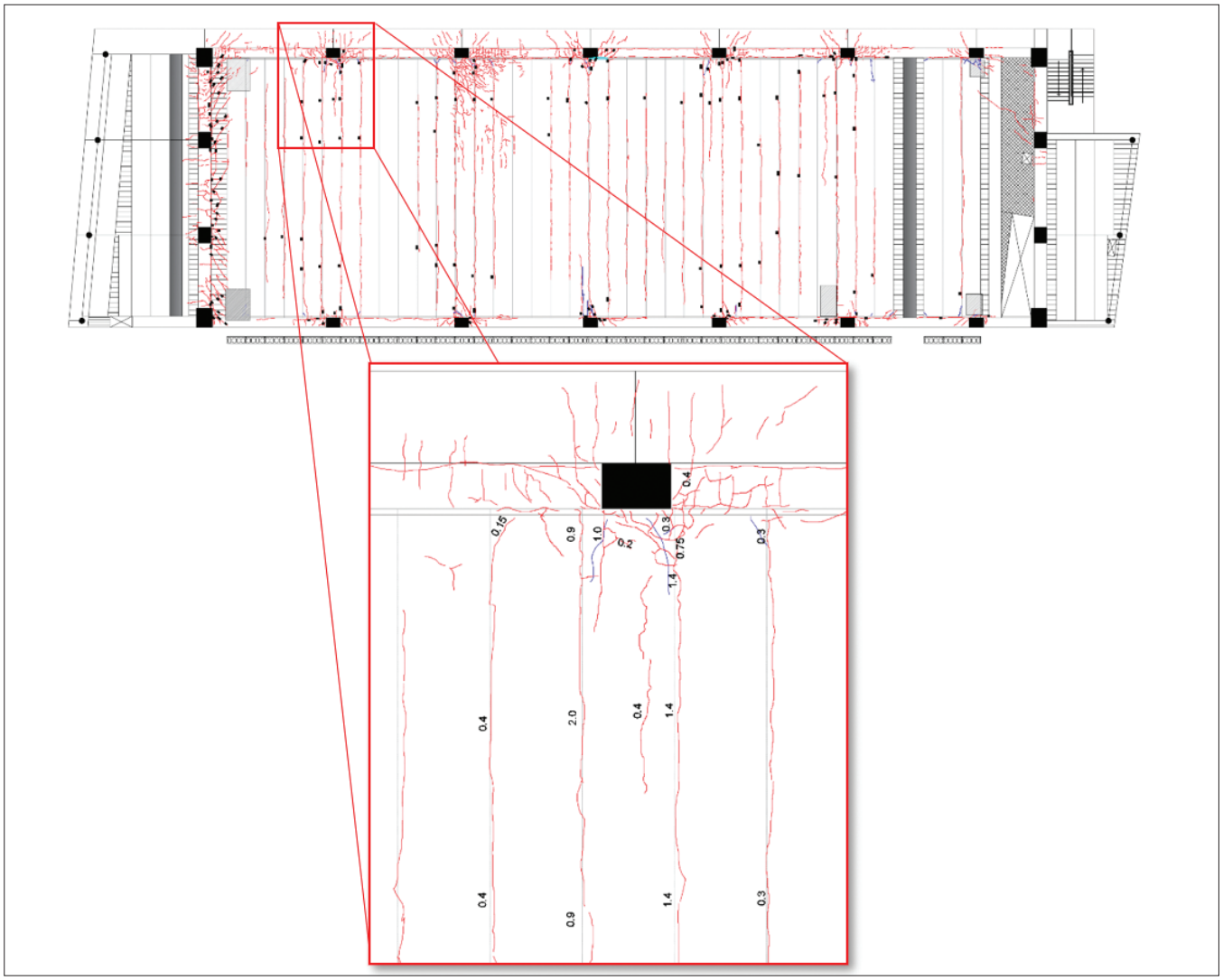

Figure 8: Crack map sample from the second floor in Pier 3 with floor top cracking marked in red, soffit cracks marked in blue,

zones was observed in multiple locations in the building (e.g. Figure 9). However, no loss of unit support was observed due to the ledge reinforcement detailing used in this building.

(a) **(b)**

Figure 9: Significant support ledge spalling observed at different locations in the building (a) Pier 3 level 1 (modified from Siddiqui et al. (2019a)) (b) Pier 2 level 1

5.2 DAMAGE TO UNIT SOFFIT

As for the hollow-core units damage observed at the soffit, a significant proportion of the hollow-core floor units in the building sustained some level of damage due to deformation incompatibilities between the hollow-core units and the supporting frames under seismic demands. The corners of the hollow-core units were found to be damaged in many units throughout the building. This corner cracking was found to occur in units regardless of their location in the building (i.e. seated over a column, within the plastic hinge zone or outside the plastic hinge zone) with various degrees of damage, as shown in Figure 10. Given the prevalence of this crack type, with evidence of grout seeping out of one unit corner crack in the building (Figure 11a), this corner cracking is also being observed in buildings located in Auckland that have not been subjected to earthquake loading (Figure 11b). These corner cracks were likely caused by non-seismic damage. Such damage could have occurred during production due to the saw-cut not being deep enough, the saw blade binding when the member cambers, or uneven handling due to pick-up devices not being level (Hoisington et al. 1983).

Another reason for this cracking could be damage initiation during construction, in which the units are usually placed on their side first while installing them in their final location. This installation method could place localized stress on the corners of the units at the supports resulting in the observed cracking. While it is likely these corner cracks were initiated during the production or construction phases, it is expected that these corner cracks opened up during the earthquake and propagated through one or two webs, reducing the shear capacity of the units. Moreover, where the side of the units was visible, it was found that the corner cracking observed from the bottom of the units propagated through the external web of the unit (Figure 10c). Corner cracking propagation through the external webs could not be confirmed for units seated within the middle of the floor (Figure 10a and Figure 10b).

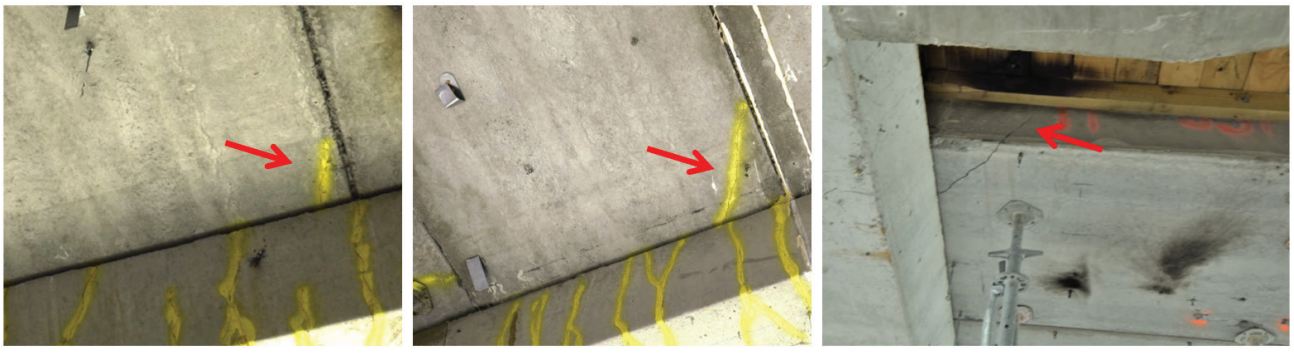

(a) (b) (c)

Figure 10:(a) minor hairline corner crack (b) Moderate corner crack (c) corner cracking propagating through exterior web when visible

(a) (b)

Figure 11: (a) corner crack with grout seeping out observed in the building investigated (b) corner crack observed in a carpark in Auckland

In addition to the corner cracking in the soffit of the units, longitudinal cracking in the bottom flange of the hollow-core units was also observed in multiple units with varying degrees of severity from hairline cracking to wide cracks that extended the full length of the unit. Longitudinal cracking might be problematic if the cracking crossed a web (Figure 12) which was typically found in units seated within the plastic hinge zone. Longitudinal cracking of units seated within the plastic hinge region occurs due to the deformation of the supporting beam under seismic demands and can be accompanied by web splitting that may result in the separation of the unit's bottom half from the unit's top half. Web splitting was identified in the units seated within the plastic hinge region via borescope.

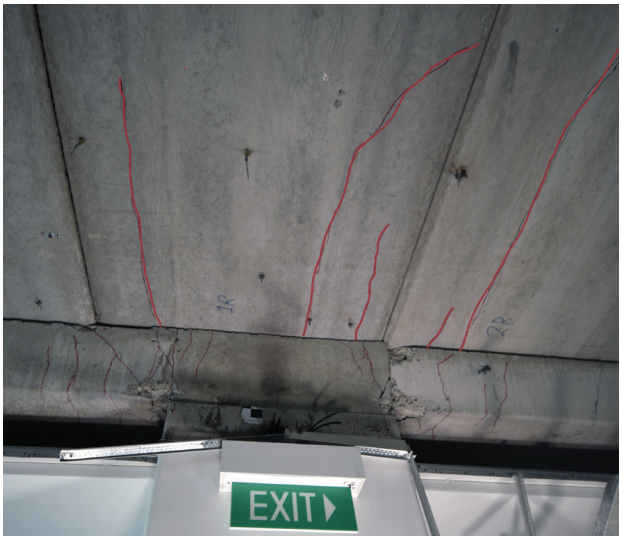

Figure 12: longitudinal cracking of HC unit soffit

Transverse cracking in the soffit of the precast hollow-core units was also observed in multiple units. Based on previous research observations (Fenwick et al. 2010), such damage indicates the propagation of cracking through the unreinforced unit webs (e.g. Figure 13a). Several floor units throughout the building were temporarily shored immediately after the earthquake as the damage observed in these units suggested that their vertical load-carrying capacity had been compromised. Moreover, web cracking was evident in units where the side of the hollow-core unit was visible, with no signs of damage observed at the unit's soffit (Figure 13b). Such observations not only reinforce the concerns regarding the risk these floors possess - given the inability to inspect these webs without invasive techniques such as using a borescope - but also raise concerns regarding the efficiency of the low friction bearing strip to suppress positive moment damage. A preliminary explanation of the web damage observed (Figure 13b) would be due to the filled cores with R16 bars trapping the unit and not allowing the unit to slide over the low friction bearing strip. Furthermore, cracking of hollow-core unit's external webs was observed in multiple units where the side of the unit was visible (Figure 14). In one of these units with exposed sides, severe web cracking of approximately 30 mm was observed (Figure 14b).

(a)

(b)

Figure 13: (a) positive moment failure in test conducted by Bull & Matthews (2003) (b) web cracking observed from unit side

(a) (b)

Figure 14: (a) transverse cracking observed at the soffit of the HC unit away from the support propagating through the web (b) HC unit corner severely damaged and unit dropping with severe web cracking (about 30 mm) propagating through the web

In addition to the units' corner, longitudinal, and transverse cracking, a damage pattern that has not been previously observed in either test specimens or other hollow-core building damage reports was observed repeatedly throughout the building. The damage pattern primarily consists of the two corners of the unit ends being cracked accompanied by a curved transverse cracking about 300 mm away from the support (Figure 15). This "transverse hoop" damage pattern was found in units seated on a column, where these units have been subjected to a combination of rotational and bending demands in both transverse and longitudinal directions of the units during the earthquake shaking. Units exhibiting this transverse hoop damage pattern were located on different floors that were subjected to different drift demands.

Finally, transverse cracking at a unit soffit accompanied by web cracking (Figure 16c) was observed at the top storey where the imposed storey drift demand was as low as 0.6% in the longitudinal direction of the unit and 1.0% in the transverse direction. Preliminary analysis suggests that diaphragm demands (Figure 16) due to higher floor accelerations may have influenced the occurrence of such damage at such low drift demands. Almost half of the floor inertial load in the longitudinal direction needs to be transferred to the moment-resisting frame through a tension tie due to the presence of a floor opening in the shown location. Although a tie beam was present, the tensile forces from the inertial loads, in addition to the relatively small deformation demands imposed on the unit from the supporting frame, was sufficient to cause the damage pattern shown in Figure 16c. Such damage highlights the challenges of ensuring good performance of hollow-core floors even when incorporated in regular floor diaphragms.

(a) (b) (c)

Figure 15: Previously unidentified repeated damage pattern highlighted in red (a) Pier 2 level 4 (b) Pier 3 level 2 (c) Pier 2 level 3

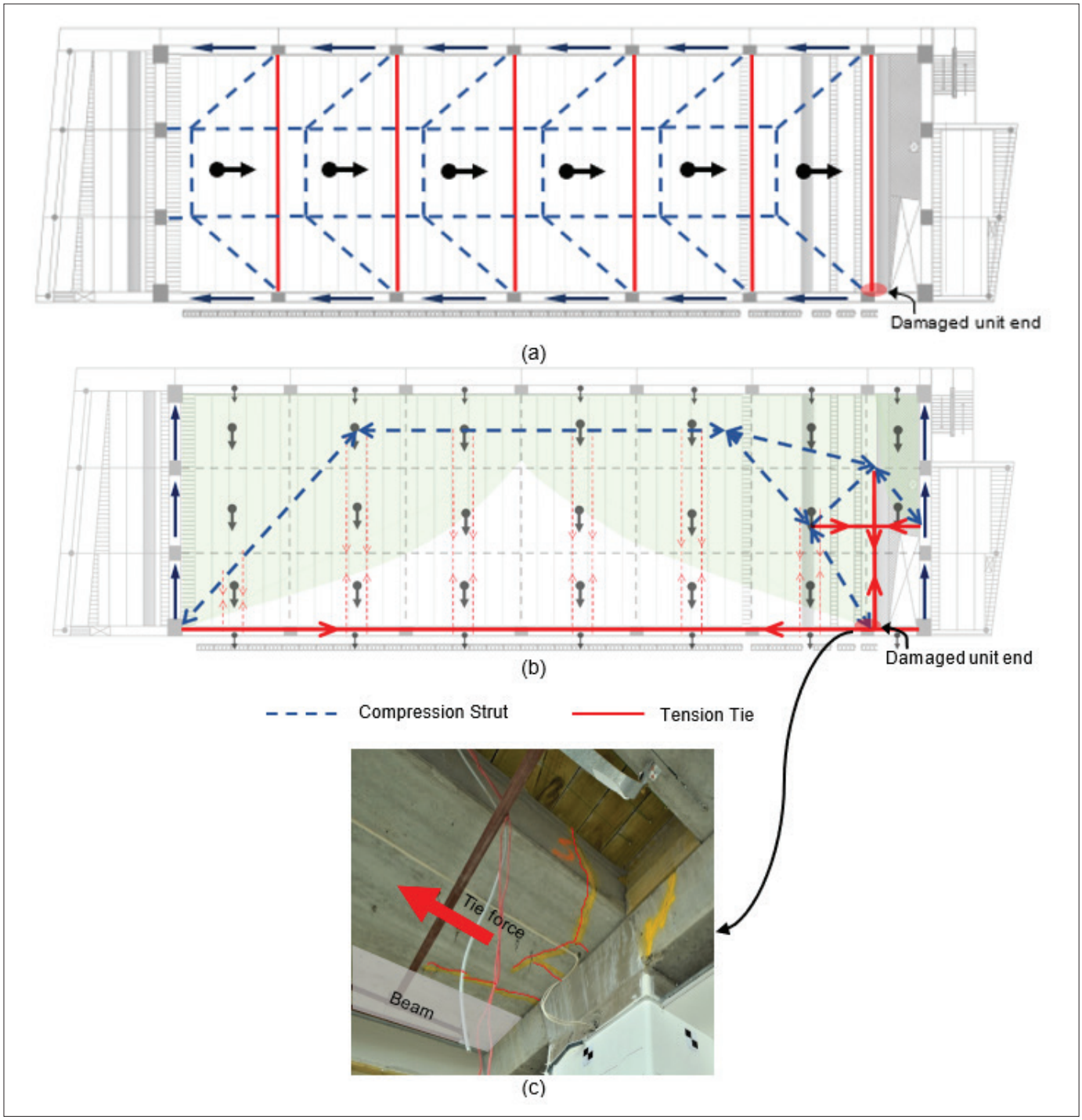

Figure 16: Simplified Strut and Tie (S-T) model for diaphragm inertial forces and damage observed at top storey with low drift demands highlighted in red, (a) S-T model for inertial loads in the transverse direction (b) S-T model for inertial loads in the longitudinal direction (c) damage observed in hollow-core unit at top storey

5.3 FLOOR DAMAGE CLASSIFICATION

Various degrees of hollow-core units damage were observed throughout the building, from insignificant hairline cracking to very wide cracking reaching approximately 30 mm. To quantify the extent of damage sustained in the floors, a qualitative framework was developed to classify different observed damage states. Table 1 summarises the approach used to quantify observed floor damage. Using the defined framework, the observed damage state at each floor unit was qualitatively assessed, and a damage state was assigned to each hollow-core unit.

The inspection of the floor units was only possible from the soffit. Hence the categorisations of the damage sustained in the hollow-core units primarily relied on the inspection of the floor unit's soffit. There was a degree

of engineering judgement involved in interpreting the significance of different damage states, and as such, some potential variance in evaluations can result. However, the interpretation of damage severity was based on available research information on the seismic performance of these floors (Bull et al., 2009; Fenwick et al., 2010). According to the classification criteria defined herein, the damage severity for each end of the hollow-core units was mapped for each floor. An example is shown in Figure 17. Then the damage severity for each end of the hollow-core units was plotted against each unit location relative to the nearest column for 684 unit-ends (i.e. 342 units) (Figure 18). It was noted that there was a trend for the damage severity, where the closer the unit was to a column, the higher the degree of damage. More severe damage was found in units seated either fully or partially on a column (referred to as 'beta units'), where the precast floor units were subjected to localised deformation to accommodate the deformation of the supporting seismic and gravity systems. These observations highlighted the susceptibility of hollow-core floor units to sustain a higher degree of damage when seated within the plastic hinge regions. The plastic hinge length was taken as half of the supporting beam depth (effective plastic hinge length ~0.5h_b, according to the yellow chapter-C5).

Table 1: Summary of damage quantification framework used to assess different floor damage states

Damage State	Damage Index	Description	Possible damage patterns
No Damage	0	No visible damage	-
Light Damage	1 2	Damage that is expected to have generally not compromised the units' gravity load carrying capacity	• Hairline longitudinal cracking. • Corner crack crossing the external web only. • Minor local support ledge spalling.
Moderate Damage	3	Damage that has potentially compromised the gravity load carrying capacity	• Visible longitudinal cracking of units. • Large corner cracking crossing more than one web. • Hairline web cracking (no risk of losing load path), visible in units beside link slabs. • Moderate support ledge spalling.
Heavy Damage	4	Damage that has compromised the units' capacity and a reliable load path is lost and/or possesses the risk of collapse in an aftershock	• Soffit transverse cracking. • Soffit diagonal cracking (not corner crack). • Web cracking. • Reduced floor support (significant support ledge spalling).

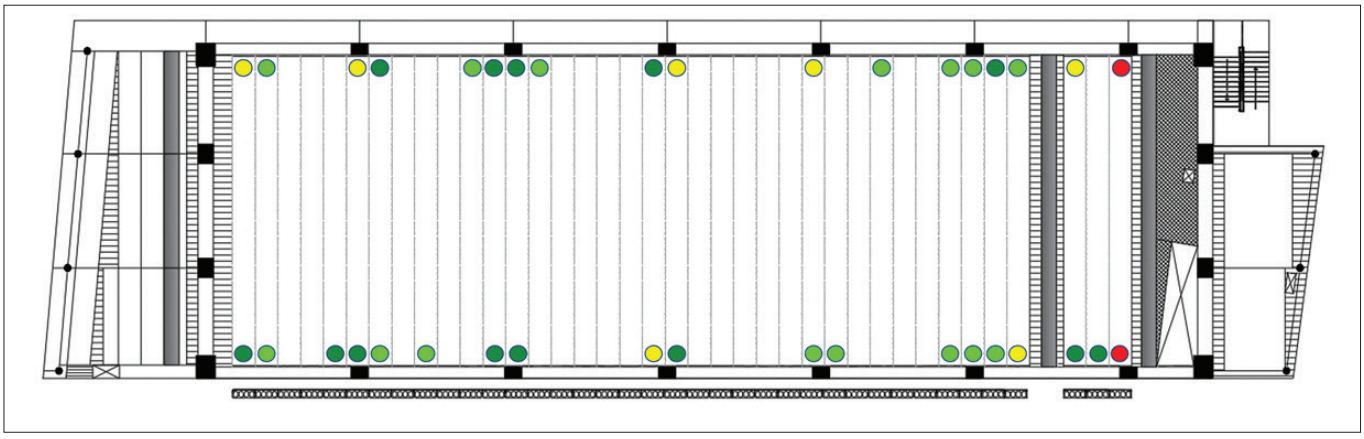

Figure 17: Floor damage distribution example, Pier 3 - level 2

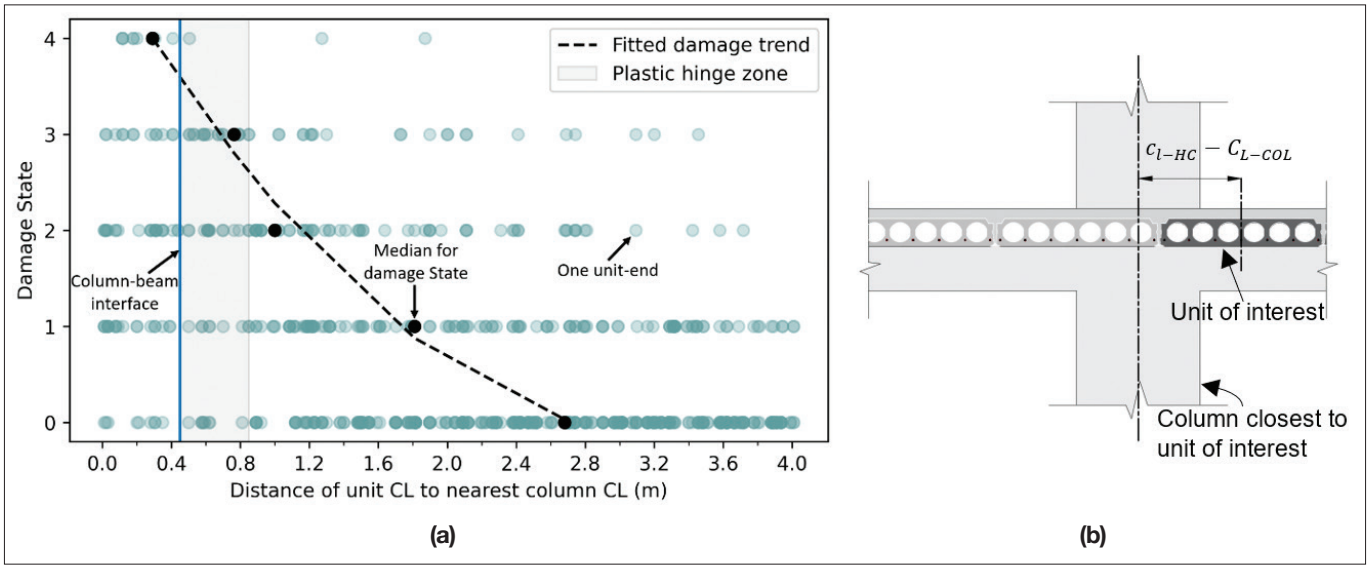

Figure 18: (a) Damage severity trend relative to unit location (centreline of unit relative to centreline of nearest column) (b) illustrative schematic of the units' location used

6 CONCERNS

The observations discussed above raise the following concerns regarding the expected seismic performance of hollow-core floors in future earthquakes:

- The susceptibility of hollow-core floor units to sustain a higher degree of damage when seated within the plastic hinge regions of the supporting beam or within the column depth ('beta' units) is neither recognised in the current design standard, NZS3101:2006-A3 (Standards New Zealand 2017), nor in the Yellow Chapter of the Assessment Guidelines C5 (MBIE et al. 2018).
- The seating detail (Figure 2) is consistent with C18.6.7(e) of NZS3101:2006-A3, which is referenced within clause 3.1.1 of B1/VM1, and hence, can be considered a deemed-to-comply solution meeting the performance objectives of the Building Code. However, the damage reported above suggests that this detail does not result in performance consistent with the life safety and amenity performance objectives of the Building Code.
- Inertial forces in the diaphragm can cause additional unintended tensile forces in hollow-core units which can lead to unit damage at lower-than-expected drifts.
- The assessment guidelines do not treat beta units differently from any other units and consequently an engineer may miss identifying the vulnerability of these units, potentially leading to a retrofit design which does not fully address the higher risks posed by such units (Mostafa et al. 2022a).

7 CONCLUSION

The major floors damage observations of a case study building with hollow-core floors subjected to design-level ground shaking during the 2016 Kaikoura Earthquake have been presented in this paper. Poor and unexpected performance of precast hollow-core floor units designed according to the current design standard, NZS 3101:2006-A3, was observed. Heavy damage was primarily found in hollow-core units seated either fully or partially on a column, where the precast floor units were subjected to localised deformations to accommodate the deformation of the supporting seismic and gravity systems. A hollow-core unit with transverse soffit cracking and web cracking was observed at the top floor with storey drift levels of approximately 0.6% and 1% longitudinal and transverse to the unit direction, respectively. Preliminary analysis suggests that diaphragm demands due to higher upper-storey floor accelerations may have influenced the occurrence of such damage at such low drift demands. A previously unidentified damage pattern, including both soffit and web cracking, was also repeatedly observed. The observed damage patterns are not directly accounted for in the assessment procedures of the Yellow Chapter of the Assessment Guidelines (MBIE et al. 2018).

Despite the above concerns, the seating detail did suppress the classical hollow-core seismic failure modes (i.e. loss of seating, positive moment failure, and negative moment failure). While significant support ledge spalling was observed, the ledge reinforcement detailing used in this building provided sufficient support length after

spalling. Negative moment failure was not observed. Classical positive moment failure was not observed, albeit transverse cracking at the soffit was observed in association with other forms of damage reported above. No ductile mesh rupture was observed, despite the diaphragm sustaining residual crack widths of approximately 7 mm. The frame damage observed was moderate and generally considered to be repairable.

Based on the observations discussed herein, SESOC, NZSEE, and Engineering NZ have recently advised that "the use of hollow-core floors in new buildings is not considered to represent good structural engineering practice and therefore we do not recommend its use" (SESOC et al. 2021). Furthermore, MBIE is currently initiating public consultation on changes to B1/VM1 such that the seating detail in Figure C18.4 NZS 3101:2006-A3 will not be considered a deemed-to-comply solution.

8 ACKNOWLEDGEMENT

This investigation is supported by the Building Research Association of New Zealand (BRANZ) under Grant No. LR13069 and ReCast project. Thanks goes to Dr. Andrew Stolte and Dr. Max Stephens for their help collecting the data and the Natural Hazards Engineering Research Infrastructure (NHERI) RAPID Facility for providing the BLK360 scanners. The authors would like to thank Prof. Des Bull for his feedback and review of this paper and Will Parker for reviewing this paper.

9 REFERENCES

Boore, D. M., and Bommer, J. J. 2005. "Processing of Strong-Motion Accelerograms: needs, options and consequences." Soil Dynamics and Earthquake Engineering, 25 (2): 93–115. https://doi.org/10.1016/j.soildyn.2004.10.007.

Bradley, B. A., Razafindrakoto, H. N. T. and Polak, V. 2017. "Ground-Motion Observations from the 14 November 2016 M_w 7.8 Kaikoura, New Zealand, Earthquake and Insights from Broadband Simulations." Seismological Research Letters, 88 (3): 740–756. https://doi.org/10.1785/0220160225.

Bull, D. K., Fenwick, R., Fulford, R., Jury, R., Hopkins, D., Lawrance, G., McSaveney, L., Pampanin, S., Smith, A. and Smith, P. 2009. Seismic Performance of Hollow Core Floor Systems Guidelines for Design Assessment and Retrofit.

Bull, D., and Matthews, J. 2003. Proof of Concept Tests for Hollowcore Floor Unit Connections. 84. Research Report. New Zealand: University of Canterbury.

Corney, S., Puranam, A., Elwood, K. J., Henry, R. S. and Bull, D. 2021. "Seismic Performance of Precast Hollow-Core Floors: Part 1—Experimental Data." SJ, 118 (5). https://doi.org/10.14359//51732821.

CSI Limited. 2017. "CUSP-Ms RS422 Structural Monitoring System Technical Manual."

Dominion Post. 2013. "BNZ Harbour Quays building Closed After Quake." 2013.

Fenwick, R., Bull, D. and Gardiner, D. 2010. Assessment of Hollow-Core Floors for Seismic Performance. 152P. Research Report. New Zealand: University of Canterbury.

GeoNet. 2013a. "M_w 6.5 Cook Strait Sun, Jul 21 2013." Accessed June 22, 2021. https://www.geonet.org.nz/earthquake/technical/2013p543824.

GeoNet. 2013b. "M_w 6.6 Lake Grassmere Fri, Aug 16 2013." Accessed June 22, 2021. https://www.geonet.org.nz/earthquake/technical/2013p613797.

GeoNet. 2016. "M_w 7.8 Kaikōura Mon, Nov 14 2016." Accessed June 22, 2021. https://www.geonet.org.nz/earthquake/technical/2016p858000.

Hamling, I. J., Hreinsdóttir, S., Clark, K., Elliott, J., Liang, C., Fielding, E., Litchfield, N., Villamor, P., Wallace, L., Wright, T. J., D'Anastasio, E., Bannister, S., Burbidge, D., Denys, P., Gentle, P., Howarth, J., Mueller, C., Palmer, N., Pearson, C., Power, W., Barnes, P., Barrell, D. J. A., Van Dissen, R., Langridge, R., Little,T., Nicol, A., Pettinga, J., Rowland, J. and Stirling, M. 2017. "Complex Multifault Rupture During the 2016 M_w 7.8 Kaikōura Earthquake, New Zealand." Science, 356 (6334): eaam7194. https://doi.org/10.1126/science.aam7194.

Hasan, M. D., Ahmad, Z. A. B., Leong, M. S. and Hee, L. M. 2018. "Enhanced Frequency Domain Decomposition Algorithm: A Review of a Recent Development for Unbiased Damping Ratio Estimates." Journal of Vibroengineering, 20 (5): 1919–1936.

Henry, R. S.,Dizhur, D., Elwood, K. J.,Hare, J. and Brunsdon, D. 2017. "Damage to Concrete Buildings With Precast Floors During The 2016 Kaikoura Earthquake." BNZSEE, 50 (No.2): 174–186.

Hoisington, R. W., Rabbat, B. G., Clark,T. H., Nijhawan, J. C., Coenen, V., Patel, I. C., Stephen, D. D., Scalia, D., Henry, J. B., Snow, J. D. and Sturm, E. R. 1983. "Fabrication and Shipment Cracks in Prestressed Hollow-Core Slabs and Double Tees." PCI journal, 28 (1).

Kaiser, A., Balfour, N., Fry, B., Holden, C., Litchfield, N., Gerstenberger, M., D'Anastasio, E., Horspool, N., McVerry, G., Ristau, J., Bannister, S., Christophersen, A.,Clark, K., Power, W., Rhoades, D.,Massey, C., Hamling, I., Wallace, Mountjoy, L. J., Kaneko Y., Benites, R., Van Houtte, C., Dellow, S., Wotherspoon, L., Elwood, K. and Gledhill, K. 2017. "The 2016 Kaikōura, New Zealand, Earthquake: Preliminary Seismological Report." Seismological Research Letters, 88 (3): 727–739. https://doi.org/10.1785/0220170018.

Lindsay, R. 2004. "Experiments On The Seismic Performance Of Hollow-core Floor Systems In Precast Concrete Buildings." Masters of Engineering. Christchurch, New Zealand: University of Canterbury.

MacPherson, C. 2005. “Seismic Performance And Forensic Analysis Of a Precast Concrete Hollow-core Floor Super-assemblage.” Masters of Engineering. Christchurch, New Zealand: University of Canterbury.

MBIE. 2021. Acceptable Solutions and Verification Methods For New Zealand Building Code Clause: B1 Structure. New Zealand: Ministry of Business, Innovation and Employment.

MBIE, EQC, NZSEE, SESOC, and NZGS. 2018. “Technical Proposal to Revise the Engineering Assessment Guidelines- PART C5 -Concrete buildings.” The Seismic Assessment of Existing Buildings. New Zealand.

McHattie, S. A. 2013. “Seismic Response of The UC Physics Building in The Canterbury Earthquakes.” New Zealand: University of Canterbury.

Mostafa, M., Büker, F., Hogan, L. S., Elwood, K. J. and Bull, D. 2022a. “Seismic Performance of Precast Hollow-core Units Seated Within the Plastic Hinge Region.” New Zealand Society for Earthquake Engineering. New Zealand: Proceedings of the 2022 NZSEE Annual Technical Conference.

Mostafa, M., Hogan, L. S., Stephens, M., Olsen, M. J. and Elwood, K. J. 2022b. “A Detailed Damage Investigation of an Instrumented Building Damaged During the M_w 7.8 Kaikoura Earthquake (In development).” Earthquake Spectra.

Peeters, B., and De Roeck, G. 1999. “Reference-Based Stochastic Subspace Identification for Output-Only Modal Analysis.” Mechanical Systems and Signal Processing, 13 (6): 855–878.

Puranam, A., S. Corney, Elwood, K. J., Henry, R. S., and Bull, D. 2021. “Seismic Performance of Precast Hollow-Core Floors: Part 2—Assessment of Existing Buildings.” SJ, 118 (5). https://doi.org/10.14359/51732822.

Seismosoft. 2016. SeismoSignal - A computer program for signal processing of time-histories.

SESOC, NZSEE, and ENZ. 2021. “Advice on Hollow-core Floors.” Accessed January 22, 2022. https://www.sesoc.org.nz/precast-flooring-resources/.

Siddiqui, U., Parker, W., Davey, R. and Therkleson. S. 2019a. “Seismic Response of BNZ Building in Wellington Following The 2016 Kaikoura Earthquake.” Auckland, New Zealand.

Siddiqui, U., Parker, W., Davey, R., Therkleson, S. and Ma., Q. 2019b. “Methodologies to Assess and Quantify Earthquake Damage: A Damage Assessment Case Study of The BNZ Building in Wellington Following The 2016 Kaikoura Earthquake.” Auckland, New Zealand.

Standards New Zealand. 2016. Structural design actions. New Zealand Part 5, Part 5. (NZS 1170.5).

Standards New Zealand. 2017. Concrete structures standard. Part 1: The Design of Concrete Structures. Part 2: Commentary on the Design of Concrete Structures. (NZS 3101.1:2006 & NZS 3101.2:2006).

Uma, S. R., King, A.,Cousins, J. and Gledhill,K. 2011. “The Geonet Building Instrumentation Programme.” NZSEE, 44 (1): 53–63.

Van Houtte, C., Bannister, S., Holden, C., Bourguignon, S. and McVerry, G. 2017. “The New Zealand Strong Motion Database.” NZSEE, 50 (1): 1–20.

SESOC SOFTWARE

Software can be found on the SESOC Webpage: sesoc.org.nz/software/.

MemDes NEW UPDATE

MemDes – Version v4.0 is now available on the SESOC website. Improvements include:

- Customised properties for standard sections
- User and project libraries of saved custom sections
- User-specified fy for custom welded beams
- Output calculations to PDF; improved calculation formatting
- Batch mode allowing multiple analyses in a single run
- Various technical and UI improvements.

SOFTWARE LICENSE ACTIVATION

- The SESOC License Key can now be found on the SESOC webpage. Details on how to activate software can be found at https://www.sesoc.org.nz/software/licensing-support/
- Please note that SESOC allows members two activations each, eg one in the office, and one at home.
- However, when upgrading a PC the user is advised to uninstall each of the SESOC software programs from off the old PC – this will release the activation back to the pool, otherwise contact software@SESOC.org.nz to remedy the problem.

ISSN No. 2744-7871